



## Computational design and performance prediction of carbazole–triazine-based TADF emitters

Ayhan Üngördü<sup>1,a,\*</sup>

<sup>1</sup> Department of Chemistry, Faculty of Science, Sivas Cumhuriyet University, Sivas, Türkiye.

\*Corresponding author e-mail address: [aungordu@cumhuriyet.edu.tr](mailto:aungordu@cumhuriyet.edu.tr)

### Research Article

#### History

Received: 09.12.2025

Accepted: 12.04.2026



This article is licensed under a Creative Commons Attribution-NonCommercial 4.0 International License (CC BY-NC 4.0)

### ABSTRACT

There are challenges in the development of organic light-emitting diode (OLED) technologies that aim to develop highly efficient, cost-effective, and stable blue thermally activated delayed fluorescent (TADF) emitters. This computational chemistry study presents a comprehensive theoretical investigation of the photophysical, electronic, and charge transport features of carbazole–triazine-based compounds to evaluate their potential for TADF applications. All geometry optimizations and excited-state calculations were carried out utilizing Density Functional Theory (DFT) and Time-Dependent Density Functional Theory (TDDFT) methods at the B3LYP/TZ2P level. The theoretical data presented suggests that substituent effects are crucial in tuning the OLED behaviors of these emitters. Furthermore, the computational evidence suggests that the investigated compounds exhibit the strong charge transfer character and the small singlet-triplet energy gap, indicating the most favorable conditions for efficient TADF emitters. The study is expected to provide guidance for TADF OLEDs formed with pure organic molecules.

**Keywords:** Carbazole–triazine based compounds, Computational chemistry, OLED design, TADF emitter, TDDFT.

<sup>a</sup> 0000-0002-7543-8379

### 1. Introduction

The search for high-efficiency and low-cost display and lighting technologies has brought organic light-emitting diodes (OLEDs) to the forefront of academic and industrial researchers[1]. In particular, following the 25% efficiency limitation of first-generation fluorescent OLEDs, the emergence of second-generation phosphorescent OLEDs with 100% efficiency has been a driving force in the development of OLED technologies[2]. Despite the high efficiency of phosphorescent OLEDs, their requirement for expensive noble metals such as iridium or platinum has driven OLED researchers to seek new, inexpensive, and highly efficient OLEDs[3]. Ultimately, these efforts have led to the emergence of third-generation thermally activated fluorescent (TADF) OLEDs, which achieve 100% efficiency without requiring expensive metals, opening a new chapter in the development of OLED technologies[4].

The principle of the TADF mechanism is based on minimizing  $\Delta E_{ST}$ , the energy difference between the lowest energy singlet ( $S_1$ ) and triplet ( $T_1$ ) excited states[5]. A small  $\Delta E_{ST}$  facilitates an efficient reverse inter-system crossing (RISC) process at room temperature using thermal energy[6]. This situation can best be achieved with molecular designs that provide a spatial separation between the highest occupied molecular orbital (HOMO) and the lowest unoccupied molecular orbital (LUMO)[7]. A proven approach to this goal is the creation of donor-acceptor (D-A) molecular architectures in which the donor

(electron-donating) and acceptor (electron-withdrawing) units are linked in a way that minimizes orbital overlap[8].

In this context, the carbazole unit stands out as a widely used robust donor due to its strong electron donating ability, high triplet energy and excellent hole transport properties[9,10]. Furthermore, since the design of TADF devices emitting high-energy blue light is challenging, the high triplet energy of carbazole is crucial for maintaining blue emission[11,12]. It is well known that triazine is a six-membered heterocyclic aromatic ring with three nitrogen atoms at its center[13,14]. This structure of triazine makes it a valuable acceptor due to its high electron affinity and thermal stability[15]. Thanks to the excellent acceptor properties of triazine, highly efficient TADF systems can be formed, especially when combined with good donor groups such as carbazole[16,17]. However, it should be noted that molecular architecture, including the number of donor units, their binding positions, and the nature of the linkers between molecules, critically determines photophysical properties such as  $\Delta E_{ST}$ , photoluminescence quantum yield, and emission color[18].

On the other hand, carbazole is structurally an electron-rich molecule. This makes it a good hole carrier[19]. In contrast, triazine has the opposite character to carbazole. Due to the electronegative nitrogen atoms in its structure, it is an electron-deficient molecule[20]. This makes it an excellent electron transporter[21]. A combined D-A system consisting of a carbazole and a

triazine group enables balanced charge transfer and injection[22,23]. This also makes combined carbazole-triazine structures important for applications such as OLEDs, where charge transport performance is critical[24, 25].

This purely computational study presents a detailed theoretical investigation and performance prediction of previously synthesized carbazole-triazine-based compounds (Ref. 26), with particular emphasis on charge transport, reorganization energies, ISC/RISC rate constants, and solvent effects, which were not comprehensively addressed in the original study.

The present study builds upon the carbazole-triazine-based compounds previously reported in [26], whose molecular structures are illustrated in Figure 1, by providing a comprehensive theoretical analysis of their photophysical and charge transport properties, with particular emphasis on singlet-triplet energy gaps, reorganization energies, and ISC/RISC rate constants.

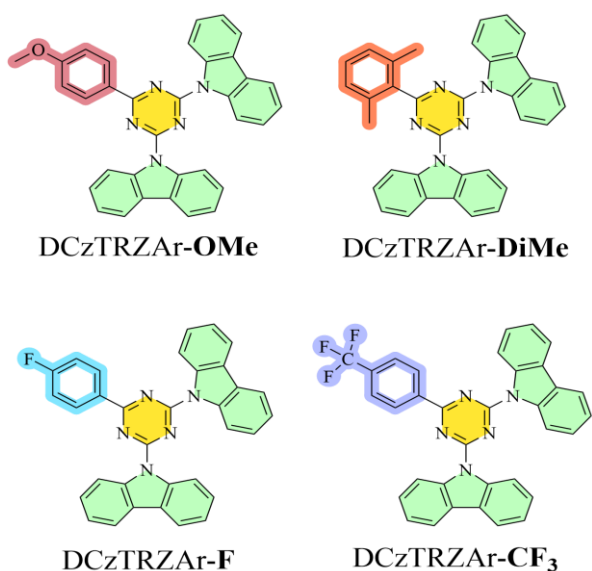


Figure 1. 2D demonstration of the carbazole-triazine based molecules studied

## 2. Materials and Methods

Density Functional Theory (DFT) and Time-Dependent Density Functional Theory (TD-DFT) computations were performed using the Amsterdam Density Functional (ADF) module of the Amsterdam Modeling Suite (AMS) 2025 package program[27]. The ground state ( $S_0$ ) and excited state ( $S_1$  and  $T_1$ ) structures of the compounds were optimized using the hybrid B3LYP functional and the TZ2P basis set, which have proven accuracy and reliability in predicting molecular orbital energies, charge transfer, and excited state properties in  $\pi$ -conjugated organic systems. Additionally, to model solvatochromic effects and predict the absorption behavior in solution, absorption calculations were also executed at the same level of theory (B3LYP/TZ2P) using the COSMO solvation model for cyclohexane, toluene, dichloromethane, and methanol solvents[28, 29].

To evaluate the charge transport properties, the electron ( $\lambda_e$ ) and hole ( $\lambda_h$ ) reorganization energies were calculated using the single-point energies of optimized neutral, anionic, and cationic structures, as detailed in

previous literature[30-33]. Similarly, key quantum chemical descriptors, including adiabatic ( $IP_a$ ) and vertical ionization potentials ( $IP_v$ ), electron affinities ( $EA_a$  and  $EA_v$ ), and chemical hardness ( $\eta$ ), were obtained from the single-point energies.

For the assessment of TADF performance, key photophysical parameters such as the singlet-triplet energy gap ( $\Delta E_{ST}$ ), spin-orbit coupling matrix elements (SOCME), and reorganization energy ( $\lambda$ ) were calculated using the optimized  $S_1$  and  $T_1$  geometries. The singlet-triplet energy gap was determined as:

$$\Delta E_{ST} = E_{S_1} - E_{T_1} \quad (1)$$

The reverse intersystem crossing ( $k_{RISC}$ ) rate constant was computed as[34,35]:

$$k_{RISC} = \frac{2\pi}{\hbar} |H_{SO}|^2 \exp\left(-\frac{(\Delta E_{ST} + \lambda)^2}{4\lambda k_B T}\right) \quad (2)$$

Similarly, the intersystem crossing ( $k_{ISC}$ ) rate constant was calculated as:

$$k_{ISC} = \frac{2\pi}{\hbar} |H_{SO}|^2 \exp\left(-\frac{(\Delta E_{ST} - \lambda)^2}{4\lambda k_B T}\right) \quad (3)$$

where  $H_{SO}$  represents the spin-orbit coupling between the  $S_1$  and  $T_1$  states,  $\lambda$  is the reorganization energy,  $k_B$  is the Boltzmann constant, and  $T$  is the absolute temperature.

## 3. Results and Discussion

### 3.1 Molecular Geometry and Frontier Molecular Orbitals

The ground-state geometries of four carbazole-triazine-based molecules were optimized at the B3LYP/TZ2P level. As shown in Figure 2, all compounds adopt a bent donor-acceptor structure, where electron-donating carbazole units and an electron-accepting triazine core are connected by an aromatic bridge. This spatial configuration is essential for achieving a minimal singlet-triplet energy splitting, a prerequisite for efficient TADF.

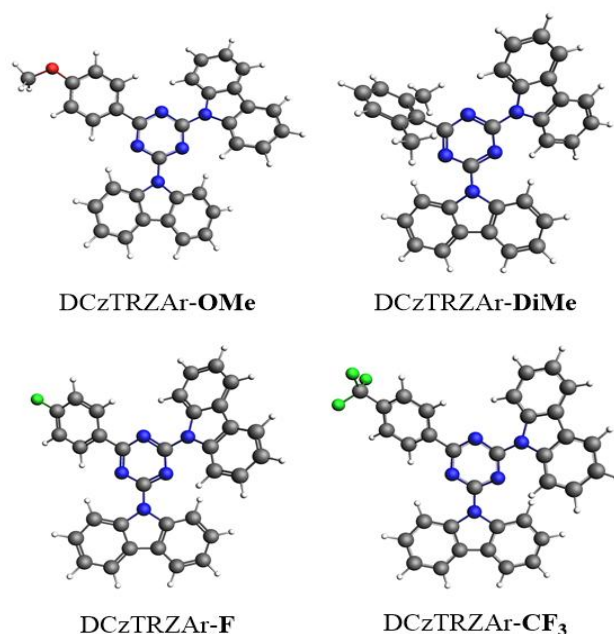


Figure 2. The optimized geometries of the carbazole-triazine based molecules investigated at B3LYP/TZ2P level.

In addition to this, by analyzing frontier molecular orbitals (FMOs) which are specifically the highest occupied molecular orbital (HOMO) and the lowest unoccupied molecular orbital (LUMO), one can gain direct insight into the electronic structures that govern the TADF mechanism. For this purpose, the energies and distributions of the FMOs were computed at the B3LYP/TZ2P level. Their spatial distributions are visualized in Figure 3. Considering to Figure 3, it appears that there is a distinct spatial distinction between the HOMO and the LUMO in all the compounds studied. The HOMO is predominantly situated on the

carbazole units that donate electrons and the connecting aryl bridge, while the LUMO is almost exclusively present in the triazine core that accepts electrons and its attached substituents.

The distinct separation minimizes the wavefunction overlap between the HOMO and LUMO. This reduces the direct exchange energy, resulting in a minimal singlet-triplet energy gap. Therefore, molecules with this distinct spatial separation are endowed with a small singlet-triplet energy splitting, a key characteristic that enables their function as efficient TADF emitters.

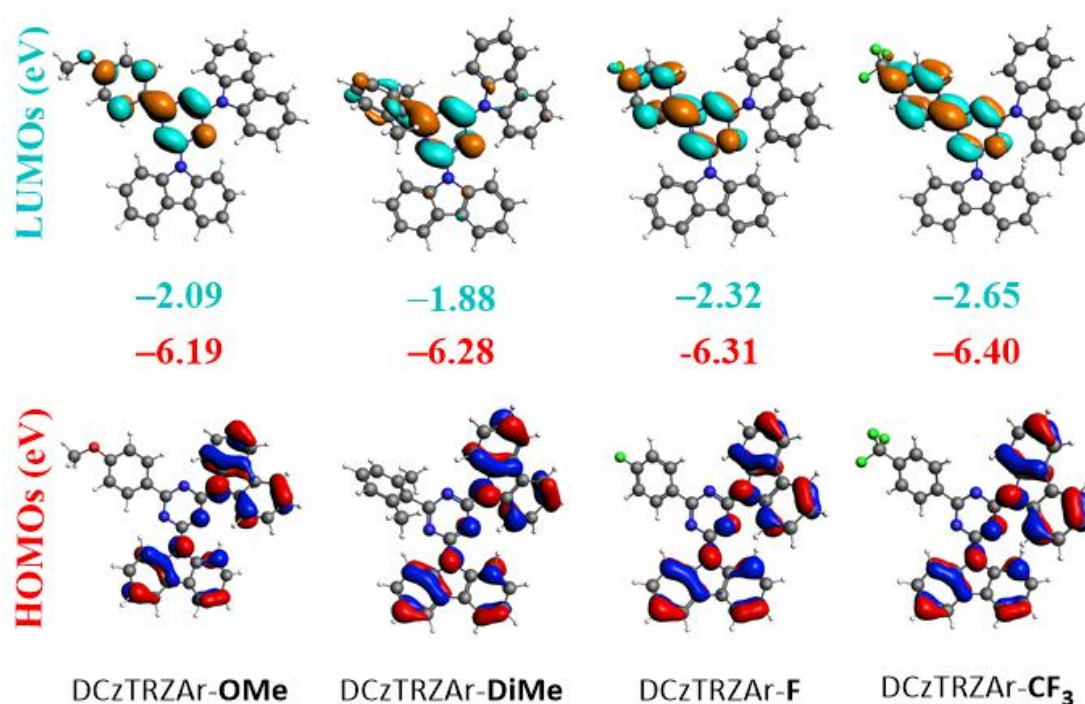


Figure 3. Calculated frontier molecular orbital distributions and energy levels of the compounds examined at the B3LYP/TZ2P level of theory in vacuum.

From Figure 3, it can be clearly shown that the HOMO energy levels range from -6.40 eV to -6.19 eV, while the LUMO energies lie between -2.65 eV and -1.88 eV. By introducing electron-withdrawing substituents (molecules 3 and 4), in particular -CF<sub>3</sub> in molecule 4, the HOMO and LUMO levels can be stabilized. Conversely, electron-donating groups (compounds 1 and 2) result in higher HOMO and LUMO levels. This controlled modulation in the FMO energies offers obvious advantages for the OLED design. The HOMO levels of the molecules 3 and 4 are ideal for matching with high-work-function anodes and thus improving hole injection. On the other hand, electron-donating molecules (1 and 2) could serve as host materials or in transport layers due to their higher-lying HOMOs, which can help block electrons and improve exciton formation. As with the HOMO level, the LUMO level needs to match the cathode. For efficient electron injection from a cathode, the energy barrier between the work function of the cathode and the LUMO level of the molecule should be minimized. Ideally, it is recommended that the cathode work function has a

greater absolute value than the LUMO energy. This enables electrons to move from the cathode to the LUMO orbital of the emissive layer in a favorable way. Referring to Figure 3, it can be expected that a low-lying LUMO, such as that in molecule 4, is optimally aligned with high-work-function cathodes.

### 3.2 Charge Transport Properties and Chemical Stabilities

Efficient and balanced charge transport is crucial for achieving high-performance OLEDs. It ensures the coordinated arrival of electrons and holes within the emission layer, thereby optimizing carrier injection and recombination across the device layers. The charge transport properties of the studied molecules are evaluated by comparing their computed reorganization energies with those of well-established standard compounds in organic light-emitting diode technology. It is well-known that Alq<sub>3</sub> (tris(8-hydroxyquinoline) aluminium) is a material that represents the standard for electron transport with a reorganization energy of 0.276 eV[36], whereas TPD (N,N'-diphenyl-N,N'-bis(3-

methylphenyl)-1,1'-biphenyl-4,4'-diamine) is utilized as the reference for hole transport, with a hole reorganization energy of 0.290 eV[37]. From Table 1, it can be shown that all of the compounds studied have electron reorganization energy values higher than the that of the standard electron transfer material, Alq3. However, from the same table, it is observed that the hole reorganization energy values of all compounds examined are lower than the that of the reference hole transfer material, TPD. Thus, one can easily state that the carbazole-triazine-based molecules investigated can be used as good hole transfer materials rather than electron transfer materials. Furthermore, it should be noted that DCzTRZAr-CF<sub>3</sub> can be proposed as an excellent candidate for hole transport material due to its lowest reorganization energy (0.07 eV) among studied molecules.

Ionization potentials (IP) and electron affinities (EA) are critical descriptors for designing efficient OLED

architecture. For efficient hole injection from the anode, it is important that the material in the adjacent hole injection layer has a low ionization energy. As shown in Table1, among the carbazole-triazine complexes studied, DCzTRZAr-OMe exhibits the lowest adiabatic and vertical ionization potential, identifying it as the most suitable candidate for the hole transfer layer. In contrast, for effective electron injection from the cathode, the material in the adjacent electron injection layer must have a high electron affinity. Based on the same table, it can be said that DCzTRZAr-CF<sub>3</sub> has the highest adiabatic electron affinity, making it the most promising candidate for the electron injection layer. Therefore, it can be predicted that an OLED stack containing DCzTRZAr-OMe in hole injection layer and DCzTRZAr-CF<sub>3</sub> in electron injection layer will provide superior charge injection.

Table 1. Computed reorganization, ionization, electron affinity, and chemical hardness energies (in eV) for the molecules studied at the B3LYP/TZ2P level of theory

Molecule	$\lambda_e$	$\lambda_h$	IP <sub>a</sub>	IP <sub>v</sub>	EA <sub>a</sub>	EA <sub>v</sub>	$\eta$
DCzTRZAr-OMe	0.28	0.14	7.04	7.11	0.97	0.69	3.04
DCzTRZAr-DiMe	0.78	0.14	7.16	7.23	0.91	0.50	3.12
DCzTRZAr-F	0.62	0.14	7.18	7.25	1.18	0.88	3.00
DCzTRZAr-CF <sub>3</sub>	0.36	0.07	7.26	7.26	1.54	1.54	2.86

$\lambda_e$  and  $\lambda_h$  denote the electron and hole reorganization energies, respectively. IP<sub>a</sub> and IP<sub>v</sub> represent the adiabatic and vertical ionization potentials, while EA<sub>a</sub> and EA<sub>v</sub> correspond to the adiabatic and vertical electron affinities.  $\eta$  is the chemical hardness.

Operational stability is the primary concern for OLED devices, along with efficiency. The chemical hardness ( $\eta$ ), a quantum chemical descriptor of molecular stability, can be utilized to estimate the relative operational lifespan of these molecules. Table 1 indicates that DCzTRZAr-OMe has the highest chemical hardness among the series, which may mean it has the most intrinsic stability and longest operational lifetime in an OLED device.

### 3.3 Photophysical Properties and TADF Performance

The main focus of this investigation is to assess the photophysical properties that pertain to TADF. The fundamental photophysical parameters, including the S<sub>1</sub>-S<sub>0</sub> and T<sub>1</sub>-S<sub>0</sub> energy gaps, the resulting fluorescence and

phosphorescence emission wavelengths, the S<sub>1</sub>-T<sub>1</sub> energy splitting, and the inter-system crossing rates (k<sub>ISC</sub>) and reverse inter-system crossing rates (k<sub>RISC</sub>), are summarized in Table 2. From the emission data in Table 2, it can be estimated that the compounds studied can predominantly emit light in the blue region (412 nm - 503 nm), based on the wavelengths corresponding to their calculated fluorescence (S<sub>1</sub>-S<sub>0</sub>) and phosphorescence (T<sub>1</sub>-S<sub>0</sub>) energies. Additionally, the calculated emission profiles of these compounds, particularly the blue fluorescence of the molecules, may contribute to solving problems associated with blue TADF emitters, which are a critical obstacle in OLED development.

Table 2. Photophysical parameters including singlet and triplet excitation energies (eV), emission wavelengths (nm), spin-orbit coupling matrix elements (cm<sup>-1</sup>), reorganization energies (eV), and intersystem crossing rate constants (s<sup>-1</sup>) for the studied molecules at 298.15 K.

Compound	S <sub>1</sub> -S <sub>0</sub>	T <sub>1</sub> -S <sub>0</sub>	Fl.	Ph.	S <sub>1</sub> -T <sub>1</sub>	SOCME S <sub>1</sub> ↔T <sub>1</sub>	$\lambda$	k <sub>RISC</sub> T <sub>1</sub> →S <sub>1</sub>	k <sub>ISC</sub> S <sub>1</sub> →T <sub>1</sub>
DCzTRZAr-OMe	2.88	2.89	430	429	0.00*	0.49	0.59	2.59 × 10 <sup>5</sup>	2.59 × 10 <sup>5</sup>
DCzTRZAr-DiMe	3.01	2.91	412	426	0.10	0.53	0.91	1.39 × 10 <sup>3</sup>	6.83 × 10 <sup>4</sup>
DCzTRZAr-F	2.74	2.71	452	457	0.03	0.10	0.06	2.83 × 10 <sup>6</sup>	9.11 × 10 <sup>6</sup>
DCzTRZAr-CF <sub>3</sub>	2.50	2.47	495	503	0.04	0.10	0.04	2.72 × 10 <sup>7</sup>	1.29 × 10 <sup>7</sup>

S<sub>1</sub>-S<sub>0</sub> and T<sub>1</sub>-S<sub>0</sub> represent the singlet and triplet excitation energies from the ground state, respectively. Fl. and Ph. denote the fluorescence (S<sub>1</sub>→S<sub>0</sub>) and phosphorescence (T<sub>1</sub>→S<sub>0</sub>) emission wavelengths.  $\Delta E_{ST}$  is the singlet-triplet energy gap defined as E(S<sub>1</sub>) - E(T<sub>1</sub>). SOCME is the spin-orbit coupling matrix element.  $\lambda$  is the reorganization energy. k<sub>RISC</sub> and k<sub>ISC</sub> are the reverse intersystem crossing and intersystem crossing rate constants, respectively. All values are reported at 298.15 K.

\*The slightly negative  $\Delta E_{ST}$  value (-0.009 eV) obtained from the calculated S<sub>1</sub> and T<sub>1</sub> energies is within the intrinsic error margin of the TD-DFT method and is therefore considered effectively zero.

Table 2 clearly shows that the singlet-triplet gaps, which are an important step for the TADF mechanism, have exceptionally small values ranging from 0.00 eV to 0.10 eV for all compounds studied. As discussed previously, the significant spatial separation of HOMO and LUMO leads to the formation of small singlet-triplet gaps. In particular, DCzTRZAr-OMe exhibits an effectively zero gap ( $\Delta E_{ST} = 0.00$  eV), while DCzTRZAr-F and DCzTRZAr-CF<sub>3</sub> show small positive values of 0.03 and 0.04 eV, respectively. These small gaps are attributed to the pronounced spatial separation of the HOMO and LUMO orbitals, which reduces the exchange interaction and facilitates reverse intersystem crossing.

The spin-orbit coupling matrix element (SOCME) is the factor that determines the efficiency of the spin-flip processes, ISC and RISC, as it measures the interaction between electronic spin and orbital angular momentum, resulting in a mixture of singlet and triplet states. The SOCME values obtained at B3LYP/TZ2P level by utilizing the triplet states of the molecules studied are tabulated in Table 2. As listed in Table 2, it is observed that the spin-orbit coupling matrix elements for these entirely organic molecules are small (0.10-0.53 cm<sup>-1</sup>), as expected in the absence of heavy atoms. This reinforces the idea that the thermal RISC pathway enabled by the small singlet-triplet gap is the primary way to populate the singlet state, rather than direct spin-orbit coupling.

The calculated  $k_{RISC}$  and  $k_{ISC}$  values show a strong dependence on both  $\Delta E_{ST}$  and reorganization energy. DCzTRZAr-CF<sub>3</sub> exhibits the highest  $k_{RISC}$  value ( $2.72 \times 10^7$  s<sup>-1</sup>), followed by DCzTRZAr-F ( $2.83 \times 10^6$  s<sup>-1</sup>), indicating efficient reverse intersystem crossing despite relatively small SOCME values. This behavior is mainly attributed to the combination of small  $\Delta E_{ST}$  and low reorganization energy, which reduces the activation barrier for the RISC process.

In contrast, DCzTRZAr-DiMe shows lower  $k_{RISC}$  values due to its larger singlet-triplet gap (0.10 eV), which increases the activation barrier for thermal up-conversion. Although DCzTRZAr-OMe exhibits a nearly zero  $\Delta E_{ST}$ , its  $k_{RISC}$  value remains moderate, suggesting that factors such as reorganization energy and coupling strength also play a significant role in determining the overall TADF efficiency.

Overall, the results indicate that all studied compounds possess favorable characteristics for TADF, particularly due to their small singlet-triplet gaps and balanced ISC/RISC rates. Among them, DCzTRZAr-CF<sub>3</sub> and DCzTRZAr-F stand out as the most promising candidates,

combining efficient reverse intersystem crossing with suitable emission properties.

### 3.4 Solvent effects on absorption

To gain insight into their solvatochromic effects, the absorption properties are examined in different solvents such as cyclohexane, toluene, dichloromethane, and methanol. The spectra obtained in solvents of different polarities at the B3LYP/TZ2P level are seen in Figure 4. According to Figure 4, DCzTRZAr-OMe has the highest absorption intensity among the four compounds, with a maximum of 325 nm. For DCzTRZAr-OMe, a significant bathochromic shift (red-shift) is observed along with an increase in oscillator strength as the solvent polarity increases from cyclohexane to methanol. Interestingly, it can be seen in Figure 4 that the DCzTRZAr-DiMe compound exhibits an opposite behavior compared to DCzTRZAr-OMe in solvents. For DCzTRZAr-DiMe, a significant hypsochromic shift (blue-shift) is observed, accompanied by a decrease in oscillator strength with solvent polarity. On the other hand, DCzTRZAr-F and DCzTRZAr-CF<sub>3</sub> exhibit weaker solvatochromic responses compared to their methoxy- and dimethyl-substituted analogs, as clearly seen in Figure 4. With the increase in solvent polarity, DCzTRZAr-F displays a slight hypsochromic shift that is accompanied by an obvious decrease in oscillator strength. It should be noted here that the greatest blue shift occurs in toluene solvent, not parallel to the increase in polarity. Similarly, DCzTRZAr-CF<sub>3</sub> shows a slight bathochromic accompanied by a decrease in absorption intensity as solvent polarity increases. These observations reveal that electronic transitions in the compounds studied vary in different environments and that in this case, the media will change the photophysical properties according to the structure of the compound.

Finally, it should be emphasized that although absorption spectra alone cannot confirm TADF behavior, the observed bathochromic and hypsochromic shifts, along with changes in oscillator strength, reflect variations in the charge-transfer (CT) character of the excited states. In donor-acceptor systems such as the carbazole-triazine compounds studied here, solvent polarity can significantly influence the stabilization of CT states, leading to changes in excitation energies. This effect is particularly important for TADF materials, as solvent-dependent modulation of CT character can alter the singlet-triplet energy gap ( $\Delta E_{ST}$ ) and consequently affect the efficiency of reverse intersystem crossing (RISC)[38].

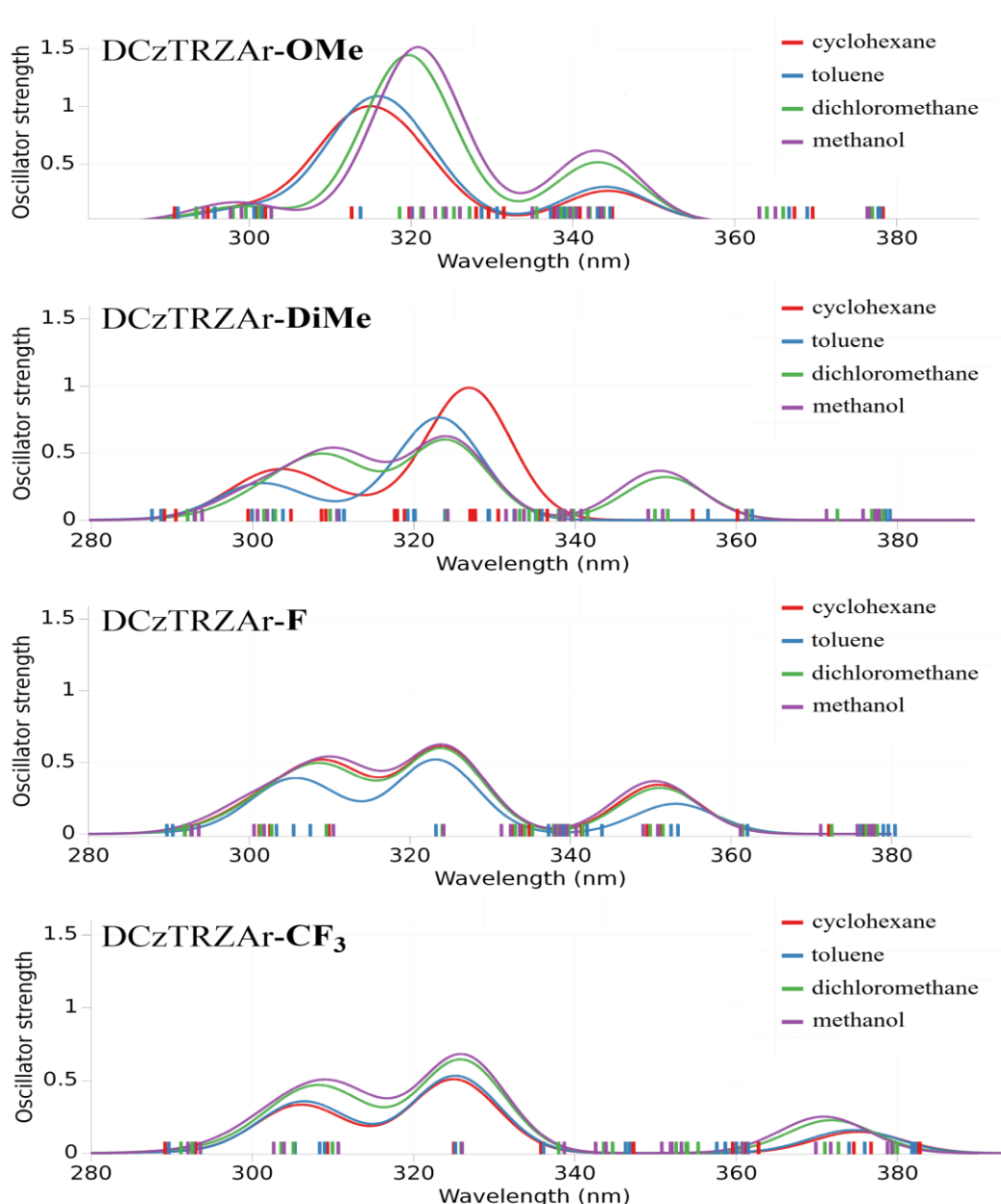


Figure 4. UV-Vis absorption spectra of the investigated organic molecules in various solvents, achieved at the TD-DFT (B3LYP/TZ2P, COSMO) level of theory.

#### 4. Conclusions

In conclusion, a comprehensive computational investigation was carried out to evaluate the TADF potential of carbazole–triazine-based donor–acceptor molecules. The results clearly demonstrate that all studied compounds exhibit a pronounced spatial separation between HOMO and LUMO orbitals, leading to extremely small singlet–triplet energy gaps ( $\leq 0.10$  eV), which is a fundamental requirement for efficient reverse intersystem crossing.

Among the investigated molecules, DCzTRZAr-CF<sub>3</sub> and DCzTRZAr-F stand out as the most promising candidates due to their favorable combination of small  $\Delta E_{ST}$  values, high  $k_{RISC}$  rates, and suitable emission characteristics in the blue region. In addition, the calculated charge transport

properties reveal that these compounds are more suitable as hole transport materials, with DCzTRZAr-CF<sub>3</sub> showing particularly low reorganization energy.

Furthermore, substituent effects were found to play a critical role in tuning the electronic structure and photophysical properties of the molecules, offering a practical strategy for the rational design of high-performance TADF emitters. Overall, this study not only predicts the promising performance of these carbazole–triazine derivatives but also provides valuable design guidelines for future development of efficient and stable blue TADF-OLED materials.

#### Conflict of Interest

There are no conflicts of interest in this work.

## References

- [1] Hong, G., Gan, X., Leonhardt, C., Zhang, Z., Seibert, J., Busch, J. M., & Bräse, S. (2021). A brief history of OLEDs—emitter development and industry milestones. *Advanced Materials*, 33(9), 2005630. <https://doi.org/10.1002/adma.202005630>
- [2] Banerjee, S., Singh, P., Purkayastha, P., & Kumar Ghosh, S. (2025). Evolution of Organic Light Emitting Diode (OLED) Materials and their Impact on Display Technology. *Chemistry—An Asian Journal*, 20(4), e202401291. <https://doi.org/10.1002/asia.202401291>
- [3] Wei, Q., Fei, N., Islam, A., Lei, T., Hong, L., Peng, R., Fan, X., Chen, L., Gao, P., & Ge, Z. (2018). Small-molecule emitters with high quantum efficiency: mechanisms, structures, and applications in OLED devices. *Advanced Optical Materials*, 6(20), 1800512. <https://doi.org/10.1002/adom.201800512>
- [4] Chen, X.-K., Kim, D., & Brédas, J.-L. (2018). Thermally activated delayed fluorescence (TADF) path toward efficient electroluminescence in purely organic materials: molecular level insight. *Accounts of Chemical Research*, 51(9), 2215–2224. <https://doi.org/10.1021/acs.accounts.8b00174>
- [5] Yersin, H., Mataranga-Popa, L., Czerwieniec, R., & Dovbii, Y. (2019). Design of a new mechanism beyond thermally activated delayed fluorescence toward fourth generation organic light emitting diodes. *Chemistry of Materials*, 31(16), 6110–6116. <https://doi.org/10.1021/acs.chemmater.9b01168>
- [6] Dos Santos, P. L., de Sa Pereira, D., Oh, C. S., Kukhta, N., Lee, H. L., Lee, J. Y., & Monkman, A. P. (2024). Influence of multiple rISC channels on the maximum efficiency and roll-off of TADF OLEDs. *The Journal of Physical Chemistry C*, 128(39), 16308–16319. <https://doi.org/10.1021/acs.jpcc.4c02993>
- [7] Song, G., He, T., Wang, R., Ouyang, Y., Jain, N., Liu, S., Kan, B., Shang, Y., Li, J., & Wang, X. (2025). Regulate the Singlet–Triplet Energy Gap by Spatially Separating HOMO and LUMO for High Performance Organic Photovoltaic Acceptors. *Angewandte Chemie*, 137(35), e202506357. <https://doi.org/10.1002/ange.202506357>
- [8] Nobuyasu, R. S., Ren, Z., Griffiths, G. C., Batsanov, A. S., Data, P., Yan, S., Monkman, A. P., Bryce, M. R., & Dias, F. B. (2016). Rational design of TADF polymers using a donor–acceptor monomer with enhanced TADF efficiency induced by the energy alignment of charge transfer and local triplet excited states. *Advanced Optical Materials*, 4(4), 597–607. <https://doi.org/10.1002/adom.201500689>
- [9] Pan, J.-H., Chiu, H.-L., & Wang, B.-C. (2005). Theoretical investigation of carbazole derivatives as hole-transporting materials in OLEDs. *Journal of Molecular Structure: THEOCHEM*, 725(1–3), 89–95. <https://doi.org/10.1016/j.theochem.2005.02.061>
- [10] Brunner, K., Van Dijken, A., Börner, H., Bastiaansen, J. J., Kiggen, N. M., & Langeveld, B. M. (2004). Carbazole compounds as host materials for triplet emitters in organic light-emitting diodes: tuning the HOMO level without influencing the triplet energy in small molecules. *Journal of the American Chemical Society*, 126(19), 6035–6042. <https://doi.org/10.1021/ja049883a>
- [11] Cai, X., & Su, S. J. (2018). Marching toward highly efficient, pure-blue, and stable thermally activated delayed fluorescent organic light-emitting diodes. *Advanced Functional Materials*, 28(43), 1802558. <https://doi.org/10.1002/adfm.201802558>
- [12] Lee, J.-H., Chen, C.-H., Lee, P.-H., Lin, H.-Y., Leung, M.-k., Chiu, T.-L., & Lin, C.-F. (2019). Blue organic light-emitting diodes: current status, challenges, and future outlook. *Journal of Materials Chemistry C*, 7(20), 5874–5888. <https://doi.org/10.1039/C9TC00204A>
- [13] Hung, W.-Y., Chiang, P.-Y., Lin, S.-W., Tang, W.-C., Chen, Y.-T., Liu, S.-H., Chou, P.-T., Hung, Y.-T., & Wong, K.-T. (2016). Balance the carrier mobility to achieve high performance exciplex OLED using a triazine-based acceptor. *ACS Applied Materials & Interfaces*, 8(7), 4811–4818. <https://doi.org/10.1021/acsami.5b11895>
- [14] Chen, H.-F., Yang, S.-J., Tsai, Z.-H., Hung, W.-Y., Wang, T.-C., & Wong, K.-T. (2009). 1,3,5-Triazine derivatives as new electron transport–type host materials for highly efficient green phosphorescent OLEDs. *Journal of Materials Chemistry*, 19(43), 8112–8118. <https://doi.org/10.1039/B913423A>
- [15] Guo, J., Zheng, C.-J., Ke, K., Zhang, M., Yang, H.-Y., Zhao, J.-W., He, Z.-Y., Lin, H., Tao, S.-L., & Zhang, X.-H. (2021). Novel triazine derivatives with deep LUMO energy levels as the electron-accepting components of exciplexes. *Journal of Materials Chemistry C*, 9(3), 939–946. <https://doi.org/10.1039/D0TC04751A>
- [16] Kang, H., Jeon, S. O., Chung, Y. S., Sim, M., Kim, J. S., Kim, J., Lee, H., Ihn, S.-G., Kim, S., & Hong, J. (2019). High-efficiency blue organic light-emitting diodes using emissive carbazole-triazine-based donor-acceptor molecules with high reverse intersystem crossing rates. *Organic Electronics*, 75, 105399. <https://doi.org/10.1016/j.orgel.2019.105399>
- [17] Zassowski, P., Ledwon, P., Kurowska, A., Herman, A. P., Lapkowski, M., Cherpak, V., Hotra, Z., Turyk, P., Ivaniuk, K., & Stakhira, P. (2018). 1,3,5-Triazine and carbazole derivatives for OLED applications. *Dyes and Pigments*, 149, 804–811. <https://doi.org/10.1016/j.dyepig.2017.11.040>
- [18] Qu, W., Gao, Z., Li, W., Fan, X., Shi, Y., Miao, Y., Wu, Z., Huang, J., Wang, H., & Wei, B. (2022). Carbazole/triazine based host materials for high-performance green PhOLEDs. *Dyes and Pigments*, 199, 110086. <https://doi.org/10.1016/j.dyepig.2022.110086>
- [19] Sathiyam, G., Sivakumar, E., Ganesamoorthy, R., Thangamuthu, R., & Sakthivel, P. (2016). Review of carbazole based conjugated molecules for highly efficient organic solar cell application. *Tetrahedron Letters*, 57(3), 243–252. <https://doi.org/10.1016/j.tetlet.2015.12.057>
- [20] Maheswari, P. U., Modec, B., Pevec, A., Kozlevcar, B., Massera, C., Gamez, P., & Reedijk, J. (2006). Crystallographic evidence of nitrate– $\pi$  interactions involving the electron-deficient 1,3,5-triazine ring. *Inorganic Chemistry*, 45(17), 6637–6645. <https://doi.org/10.1021/ic060101j>
- [21] Inomata, H., Goushi, K., Masuko, T., Konno, T., Imai, T., Sasabe, H., Brown, J. J., & Adachi, C. (2004). High-efficiency organic electrophosphorescent diodes using 1,3,5-triazine electron transport materials. *Chemistry of Materials*, 16(7), 1285–1291. <https://doi.org/10.1021/cm034689t>
- [22] Chang, C.-H., Kuo, M.-C., Lin, W.-C., Chen, Y.-T., Wong, K.-T., Chou, S.-H., Mondal, E., Kwong, R. C., Xia, S., & Nakagawa, T. (2012). A dicarbazole–triazine hybrid bipolar host material for highly efficient green phosphorescent OLEDs. *Journal of Materials Chemistry*, 22(9), 3832–3838. <https://doi.org/10.1039/C2JM14686J>
- [23] Chen, X., Zhang, X., Xiao, X., Wang, Z., & Zhao, J. (2023). Recent Developments on Understanding Charge Transfer

- in Molecular Electron Donor–Acceptor Systems. *Angewandte Chemie International Edition*, 62(16), e202216010. <https://doi.org/10.1002/anie.202216010>
- [24] Kim, M., Jeon, S. K., Hwang, S.-H., & Lee, J. Y. (2015). Molecular design of triazine and carbazole based host materials for blue phosphorescent organic emitting diodes. *Physical Chemistry Chemical Physics*, 17(20), 13553–13558. <https://doi.org/10.1039/C5CP01676B>
- [25] Li, H., Ren, H., Wang, J., Liu, D., & Li, J. (2024). Cyano Decoration of  $\pi$ -Bridge to Boost Photoluminescence and Electroluminescence Quantum Yields of Triazine/Carbazole Based Blue TADF Emitter. *Chemistry–A European Journal*, 30(4), e202303169. <https://doi.org/10.1002/chem.202303169>
- [26] El Ain, M. A., Sevilla-Pym, A., Hudson, Z. M., & Budén, M. E. (2025). Tuning the emission of carbazole-triazine based emitters through aryl substituents: towards efficient TADF materials. *Journal of Materials Chemistry C*. <https://doi.org/10.1039/D5TC01073J>
- [27] Baerends, E. J., Aguirre, N. F., Austin, N. D., Autschbach, J., Bickelhaupt, F. M., Bulo, R., Cappelli, C., van Duin, A. C., Egidi, F., & Fonseca Guerra, C. (2025). The Amsterdam modeling suite. *The Journal of Chemical Physics*, 162(16). <https://doi.org/10.1063/5.0258496>
- [28] Te Velde, G. t., Bickelhaupt, F. M., Baerends, E. J., Fonseca Guerra, C., van Gisbergen, S. J., Snijders, J. G., & Ziegler, T. (2001). Chemistry with ADF. *Journal of Computational Chemistry*, 22(9), 931–967. <https://doi.org/10.1002/jcc.1056>
- [29] Peeples, C. A., & Schreckenbach, G. (2016). Implementation of the SM12 Solvation Model into ADF and Comparison with COSMO. *Journal of Chemical Theory and Computation*, 12(8), 4033–4041. <https://doi.org/10.1021/acs.jctc.6b00410>
- [30] Üngördü, A. (2025). Theoretical study on electronic and optoelectronic properties of some C<sup>N</sup>N- and C<sup>C</sup>C-chelated iridium (III) complexes for OLEDs. *Turkish Journal of Chemistry*, 49(4), 394–403. <https://doi.org/10.1016/j.cplett.2025.142252>
- [31] Tutar, N. N., & Üngördü, A. (2025). Computational insights into the optoelectronic and electronic properties of some platinum (II) complexes for OLED applications. *Chemical Physics Letters*, 142252. <https://doi.org/10.1016/j.cplett.2025.142252>
- [32] Deng, W. Q., Sun, L., Huang, J. D., Chai, S., Wen, S. H., & Han, K. L. (2015). Quantitative prediction of charge mobilities of pi-stacked systems by first-principles simulation. *Nature Protocols*, 10(4), 632–642. <https://doi.org/10.1038/nprot.2015.038>
- [33] Marcus, R. A. (1993). Electron-Transfer Reactions in Chemistry - Theory and Experiment. *Reviews of Modern Physics*, 65(3), 599–610. <https://doi.org/10.1002/anie.199311113>
- [34] Mahaan, R., & John Bosco, A. (2023). Sulfur Oxidation State and Substituents Influenced Multifunctional Organic Luminophores in BTP Core for OLEDs: A Computational Study on RTP, TADF Emitter and Sensitizer. *The Journal of Physical Chemistry A*, 127(50), 10570–10582. <https://doi.org/10.1021/acs.jpca.3c05259>
- [35] Aizawa, N., Harabuchi, Y., Maeda, S., & Pu, Y. J. (2020). Kinetic prediction of reverse intersystem crossing in organic donor–acceptor molecules. *Nature Communications*, 11(1), 3909. <https://doi.org/10.1038/s41467-020-17777-2>
- [36] Lukyanov, A., Lennartz, C., & Andrienko, D. (2009). Amorphous films of tris(8-hydroxyquinolino) aluminium: Force-field, morphology, and charge transport. *Physica Status Solidi A*, 206(12), 2737–2742. <https://doi.org/10.1002/pssa.200925276>
- [37] Gruhn, N. E., da Silva, D. A., Bill, T. G., Malagoli, M., Coropceanu, V., Kahn, A., & Brédas, J. L. (2002). The vibrational reorganization energy in pentacene: Molecular influences on charge transport. *Journal of the American Chemical Society*, 124(27), 7918–7919. <https://doi.org/10.1021/ja0175892>
- [38] Xue, Q., & Xie, G. (2021). Thermally activated delayed fluorescence beyond through-bond charge transfer for high-performance OLEDs. *Advanced Optical Materials*, 9(14), 2002204. <https://doi.org/10.1002/adom.2002204>